crystals

MDPI

Article

Influence of Vacancy on Structural Stability, Mechanical Properties and Electronic Structures of a Ti_5Sn_3 Compound from First-Principles Calculations

Xingzhi Pang [1,2], Fenggui Wei [1], Dong Liu [3,4], Wenchao Yang [1,2], Yanjun Zhao [1,2], Jingwu Wu [3,4,*], Mingjun Pang [5] and Jianbing Yang [6,*]

1 School of Resources, Environment and Materials, Guangxi University, Nanning 530004, China; pxzh2008@gxu.edu.cn (X.P.); weifg2022@163.com (F.W.); ywch053@163.com (W.Y.); zhaoyanjun@gxu.edu.cn (Y.Z.)
2 Guangxi Key Laboratory of Processing for Non-Ferrous Metals and Featured Materials, MOE Key Laboratory of New Processing Technology for Non-Ferrous Metals and Materials, Center of Ecological Collaborative Innovation for Aluminum Industry in Guangxi, Guangxi University, Nanning 530004, China
3 The Testing and Technology Center for Industrial Products, Shenzhen Customs, Shenzhen 518067, China; 498882270@qq.com
4 Shenzhen Academy of Inspection and Quarantine, Shenzhen 518010, China
5 SAIC-GM-Wuling Automobile Co., Ltd., Liuzhou 545007, China; mjpang@163.com
6 Department of Information and Electromechanical Engineering, Guangxi Agricultural Vocational University, Nanning 530007, China
* Correspondence: wujingw@163.com (J.W.); yjbing2022@163.com (J.Y.)

Abstract: Titanium alloy is widely used in biomedical materials. Ti-Sn alloy is a new type β titanium alloy with no toxicity. In this paper, the mechanical and electronic properties of Ti_5Sn_3 with vacancy defects have been studied by using first-principles method. The vacancy formation energy, vacancy formation enthalpy, elastic constant, elastic modulus, hardness and electronic structure of perfect Ti_5Sn_3 and Ti_5Sn_3 with different vacancies were also calculated and discussed. The results show that Ti_5Sn_3 is more likely to form vacancies at V_{Ti2}. In addition, the bulk deformation resistance of Ti_5Sn_3 is weakened by the vacancy, and the shear resistance, stiffness and hardness of Ti_5Sn_3 are increased by the Ti vacancy, but the brittleness of Ti_5Sn_3 is increased. On the contrary, the presence of Sn vacancy decreases the shear resistance, stiffness and hardness of Ti_5Sn_3, and increases the toughness of Ti_5Sn_3. By analyzing the change of electronic structure, it is found that removing the Ti atom at the V_{Ti2} position can improve the interaction between atoms, while Sn vacancy can weaken the interaction.

Keywords: first-principles; vacancy; elastic properties; mechanical property; electronic structure

Citation: Pang, X.; Wei, F.; Liu, D.; Yang, W.; Zhao, Y.; Wu, J.; Pang, M.; Yang, J. Influence of Vacancy on Structural Stability, Mechanical Properties and Electronic Structures of a Ti_5Sn_3 Compound from First-Principles Calculations. *Crystals* **2022**, *12*, 1061. https://doi.org/10.3390/cryst12081061

Academic Editor: Krzysztof Szymkiewicz

Received: 25 June 2022
Accepted: 23 July 2022
Published: 29 July 2022

1. Introduction

Titanium and titanium alloys have been widely used in the field of medical orthopedic materials due to their excellent properties such as high strength, low density, corrosion resistance, lack of toxicity and good biocompatibility [1–3]. The alloy used for these applications is based on the (α + β) type titanium alloy Ti-6Al-4V (TC4). However, the elastic modulus of TC4 does not match with human bone [4–6], and it contains elements harmful to the human body [7,8]. In recent years, with the development of materials science and biology, there is a requirement for higher performance of medical titanium and titanium alloy. Therefore, β titanium alloys with high strength, low elastic modulus, lack of toxicity and good biocompatibility have attracted extensive attention from researchers. With a better understanding of the microstructure and properties of β-type titanium alloys, the application of novel β-type titanium alloys without toxicity in orthopedic materials has become possible [9].

A large number of studies have shown that the addition of a certain amount of Sn in titanium alloys can help to improve the mechanical properties of titanium alloys [3]: (i) Sn

can form solid solution strengthening in Ti, which increases the lattice parameters of Ti and increases the distance between alloy atoms [10,11]; (ii) Sn is a non-toxic element with good biocompatibility; (iii) Sn can reduce the initial martensite temperature, inhibit the formation of ω phase, and improve the elastic properties of the alloy [10,12]. Therefore, adding Sn is a good way of enhancing performance of titanium based medical orthopedic materials. In addition, Ti-Sn intermetallic compounds play an important role in improving the properties of alloys [13–18], and understanding the strengthening mechanism of intermetallic compounds is of positive significance to the study of Ti-Sn orthopedic materials. Nowadays, Ti-Sn intermetallic compounds have received more and more attention, and many studies have been conducted on the microstructure, elastic properties and phase stability of Ti_5Sn_3. For example, Tedenac et al. [19] have calculated the crystal structure and phase stability of Ti_5Sn_3 in Ti-Ni-Sn alloys by first-principles calculations. Chen et al. [20] have studied the structural stability, ideal strength and other properties of Ti_5Sn_3. Mechanical properties of solid materials are usually determined by the combination of different crystal structures and various defects (including vacancy, impurity, dislocation, etc.). Vacancy defects are inherent defects in solids and play an important role in determining the mechanical properties of solids. However, there are few studies on the physical properties of Ti_5Sn_3 and its vacancies. Therefore, the vacancy formation energy, elastic modulus, and electronic structure of Ti_5Sn_3 and Ti_5Sn_3 with different vacancies were studied by using first-principles calculations. This provides theoretical support for the design of Ti-Sn alloy.

2. Calculation Method and Model

First-principles calculations are implemented in the CASTEP module in Materials Studio based on density functional theory [21]. The correlation exchange energy between electrons is processed by the PBE function in the generalized gradient approximation (GGA) [22]. The interactions between the electrons and ion cores are employed by using an Ultrasoft pseudopotential for Ti and Sn atoms. [23]. After the convergence test, Ti_5Sn_3 truncation energy is set to 400 eV, the value of k-point in the Brillouin region is determined to be $4 \times 4 \times 4$ by the Monkhorst-Pack method, as shown in Tables 1 and 2. Geometric optimization of the established model was carried out through BFGS [24], and the most stable structure in the region was obtained. The convergence parameters of the crystal calculation process are as follows: the convergence precision of the total energy of the system is 1×10^{-5} eV/atom, the maximum Hellmann–Feynman force is 0.03 eV/Å, the maximum stress is less than 0.05 GPa, and the maximum ionic displacement is 1×10^{-3} Å. In order to confirm image–image interactions of the vacancies, the $1 \times 1 \times 1$ and $1 \times 1 \times 2$ supercell models of Ti_5Sn_3 with different vacancies were constructed in this work. The test results indicated that the effect of the periodic boundary condition is quite small, which is attributed to the distances between adjacent vacancies being at least 8 Å for the $1 \times 1 \times 1$ model of Ti_5Sn_3 with vacancies.

Table 1. Variation of total energies with different truncation energies at the same K point of Ti5Sn3.

Energy Cutoff (eV)	Total Energies (eV)
300	−16,608.69
350	−16,609.957
400	−16,610.513
450	−16,610.536
500	−16,610.538

Table 2. The K points, lattice parameters and total energies for pure Ti_5Sn_3.

K Point	a (Å)	c (Å)	E (eV)
$2 \times 2 \times 4$	8.074	5.468	−16,610.103
$3 \times 3 \times 4$	8.077	5.456	−16,610.238
$4 \times 4 \times 4$	8.081	5.449	−16,610.376
$4 \times 4 \times 6$	8.083	5.441	−16,610.404
$5 \times 5 \times 7$	8.083	5.439	−16,610.383
$6 \times 6 \times 8$	8.083	5.438	−16,610.385

The space group of Ti_5Sn_3 is P63/mcm, and the lattice constants are a = b = 8.049 Å, c = 5.454 Å, $\alpha = \beta = 90^\circ$, $\gamma = 120^\circ$ [25]. There are three kinds of atomic equivalent sites in Ti_5Sn_3 crystals, whose lattice coordinates are Ti 6g (0.230, 0, 0.250), Ti 4d (0.333, 0.667, 0) and Sn 6g (0.600, 0, 0.25), respectively. After geometric optimization, the calculated lattice parameters of Ti_5Sn_3 are a = b = 8.0805 Å and c = 5.449 Å, which are consistent with the experimental values and other theoretical results [19], which are also consistent with a = b = 8.0716 Å and c = 5.4823 Å. The original cell of Ti_5Sn_3 contains ten Ti atoms and six Sn atoms. The Ti_5Sn_3 compounds with various vacancies are obtained by removing single atoms from perfect Ti_5Sn_3 cells, then optimizing geometry again. In this way, the ground state structures of Ti_5Sn_3 with vacancies were established. Finally, the stability, electronic structure and elastic properties of the four optimized geometric structures were calculated and analyzed.

3. Results and Discussion

3.1. Structural Stability

In order to study the influence of vacancy defects on the structure and physical properties of Ti_5Sn_3, three crystal models with different vacancy defects were constructed (as shown in Figure 1), namely V_{Ti1}, V_{Ti2} and V_{Sn3}. The vacancy formation energy (E^x_{form}) determines the structural stability of vacancy defects. In order to investigate the stability of different vacancies of Ti_5Sn_3, three vacancy formation energies are calculated, and the calculation formula is as follows [26]:

$$E^x_{form} = E^x_{hole} - E^x_{host} + \mu_x \quad (1)$$

In the formula, E^x_{hole} and E^x_{host} represent the total energy of Ti_5Sn_3 with vacancy defects and Ti_5Sn_3 without defects, respectively; μ_x (x = Ti1, Ti2, Sn) represents the chemical potential of the corresponding removed atoms. The calculation of chemical potential of Ti and Sn atoms should satisfy the following equation:

$$5\mu_{Ti} + 3\mu_{Sn} = \mu^{bulk}_{Ti5Sn3} \quad (2)$$

$$\mu_{Ti} \leq \mu^{bulk}_{Ti} \quad (3)$$

$$\mu_{Sn} \leq \mu^{bulk}_{Sn} \quad (4)$$

$$\Delta H_f(Ti_5Sn_3) \leq \mu_{Ti} - \mu^{bulk}_{Ti} \leq 0 \quad (5)$$

where ΔH_f (Ti_5Sn_3) is the formation energy of a perfect Ti_5Sn_3 compound. μ^{bulk}_{Ti} and μ^{bulk}_{Sn} are the chemical potentials of Ti and Sn in the bulk perfect Ti_5Sn_3 compound.

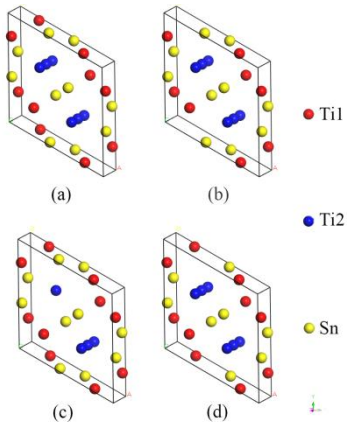

Figure 1. Crystal structure of orthorhombic Ti_5Sn_3 compounds with different vacancies: (**a**) perfect Ti_5Sn_3, (**b**) V_{Ti1}, (**c**) V_{Ti2} and (**d**) V_{Sn3}.

Obviously, the chemical potential of Ti atoms depend on the environment in which the vacancy is created. That is, the limiting cases of Sn-rich and Ti-rich. In the Ti-rich environment, μ_{Ti} approaches the chemical potential of bulk Ti, $\mu_{Ti} = \mu_{Ti}^{bulk} = -1603.122$ eV. The chemical potential of Sn can be determined from the thermochemical equilibrium condition in Equation (2), $\mu_{Sn} = (\mu_{Ti5Sn3}^{bulk} - 5\mu_{Ti}^{bulk})/3 = -96.529$ eV. In the Sn-rich environment, μ_{Sn} is close to the chemical potential of bulk Sn, $\mu_{Sn} = \mu_{Sn}^{bulk} = -95.483$ eV, $\mu_{Ti} = (\mu_{Ti5Sn3}^{bulk} - 3\mu_{Sn}^{bulk}) = -1603.750$ eV. Therefore, the formation energy variation curve of Ti_5Sn_3 with different Ti and Sn vacancies in different environments can be obtained, as shown in Figure 2.

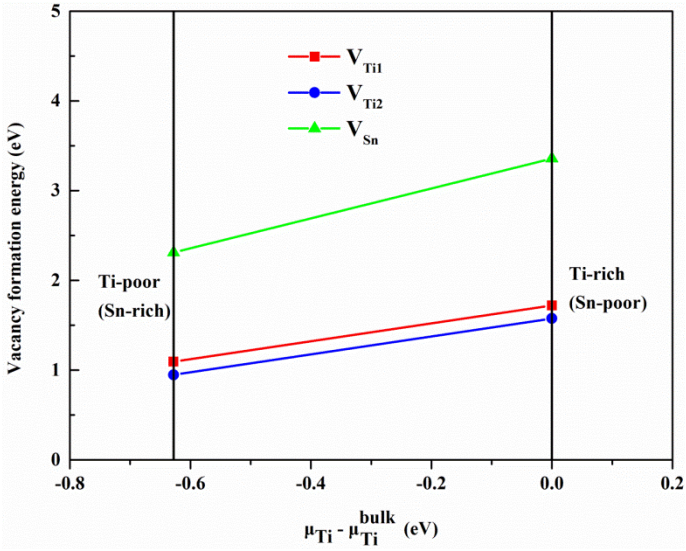

Figure 2. Vacancy formation energies of the Ti vacancy and Sn vacancy as a function of the atomic chemical potentials. The left- and right-hand sides correspond to the Sn-rich and Ti-rich compounds considered, respectively.

The lower the enthalpy of formation of a solid substance, the more stable its thermodynamic stability is. In order to study the ideal thermodynamic stability of Ti_5Sn_3 and Ti_5Sn_3 with different vacancies, the enthalpy of formation was calculated according to the given equation:

$$\Delta H(Ti_5Sn_3) = \frac{1}{x+y}\left(E_{total}(Ti_5Sn_3) - xE_{Ti} - yE_{Sn}\right) \quad (6)$$

Table 3 below lists the row forming energy and enthalpy of formation of vacant positions at three different positions. If the enthalpy of formation of a solid material is

negative, it indicates that the structure is thermodynamically stable in the ground state. It can be seen from Table 3 that the enthalpies of formation of intact Ti_5Sn_3 and different vacancy Ti_5Sn_3 are all less than zero, indicating that the Ti_5Sn_3 structures with these three vacancy defects are thermodynamically stable in the ground state. Among the three different vacancy models, the enthalpy of formation of V_{Ti2} is the smallest, indicating that the removal of Ti atoms at this position is conducive to the formation of a more stable dynamic structure. In addition, the vacancy formation energy and formation enthalpy of Ti atomic vacancy are both smaller than those of the Sn atomic vacancy, indicating that the structure of Ti_5Sn_3 with the Ti atomic vacancy in the ground state is more stable than that with the Sn vacancy. The vacancy formation energy is mainly determined by the chemical potential. The lower the vacancy formation energy, the better the dynamic stability. It can be seen from Table 3 and Figure 2 that the vacancy formation energy of V_{Ti2} is the lowest, which means that the possibility of V_{Ti2} vacancy formation is greater for Ti_5Sn_3.

Table 3. Lattice parameters, vacancy formation energy and enthalpy of formation of perfect Ti_5Sn_3 and different vacant Ti_5Sn_3.

Compound	a (Å)	b (Å)	c (Å)	E_f (eV) Ti-Poor	E_f (eV) Ti-Rich	ΔH (kJ/mol)
Ti_5Sn_3	8.0805	8.0805	5.4490			−37.536
Other [a]	8.0716	8.0716	5.4823			
Other [b]	8.0650	8.0650	5.4350			−34.870
V_{Ti1}	8.3301	7.8319	5.4883	1.094	1.722	−29.856
V_{Ti2}	7.9708	7.9704	5.4395	0.948	1.576	−31.008
V_{Sn3}	7.9322	7.9860	5.3740	2.311	3.357	−18.528

[a] Ref. [20]. [b] Ref. [27].

It can be seen from Table 3 that, compared with complete Ti_5Sn_3, the lattice constants of Ti_5Sn_3 with different vacancies show different degrees of shrinkage or expansion. The lattice constant of Ti_5Sn_3 with V_{Ti2} vacancy shrinks along the a, b and c axis lattice, which enhances the interaction between the atoms. The V_{Sn3} vacancy is the same as the V_{Ti2} vacancy, which causes lattice contraction, but there are differences between the two. It can be clearly seen from Table 3 that vacancy formation energies of Ti_5Sn_3 containing Ti vacancy defects are all lower than those containing Sn vacancy, that is, Ti atomic vacancy has a stronger stability than Sn atomic vacancy.

3.2. Mechanical Properties

The elastic property is an important aspect of the mechanical property and structural stability of materials. The elastic property of Ti_5Sn_3 is calculated by the stress–strain method. Ti_5Sn_3 has five different second-order elastic constants, and the mechanical property stability is determined by the Born criterion [28–30]:

$$\begin{gathered} C_{11} > 0, C_{33} > 0, C_{44} > 0, C_{66} > 0, C_{11} - C_{12} > 0; \\ 4C_{13} + C_{33} + 2(C_{11} + C_{12}) > 0, C_{11} + C_{33} > 2C_{13}, C_{66} = (C_{11} - C_{12})/2 \end{gathered} \quad (7)$$

The elastic constants of complete Ti_5Sn_3 and Ti_5Sn_3 with different vacancies are listed in Table 4. For the perfect Ti_5Sn_3, although there is a very small difference between the calculated elastic constants and the theoretical data for slight fluctuations, it is consistent with the theoretical results. It is not difficult to see that both intact and different vacancies of Ti_5Sn_3 show mechanical stability, because their elastic constants meet the Born stability criterion. However, the C_{11} value of intact Ti_5Sn_3 is smaller than that of intact Ti_5Sn_3 with Ti vacancy, which indicates that the existence of Ti vacancy makes the Ti_5Sn_3 crystal have stronger deformation resistance along the a-axis. On the contrary, the vacancy of Sn weakens the deformation resistance of Ti_5Sn_3 along the a-axis. In addition, the C_{33} of perfect Ti_5Sn_3 is greater than that of vacant Ti_5Sn_3. Obviously, the vacancy weakens the deformation resistance along the c-axis. In addition, the C_{44} and C_{66} of Ti_5Sn_3 with Ti

vacancy are greater than that of perfect Ti_5Sn_3, which indicates that the existence of the Ti vacancy enhances the shear resistance of Ti_5Sn_3. On the contrary, the Sn vacancy weakens the shear resistance of Ti_5Sn_3.

Table 4. Elastic constant C_{ij} (GPa) of Ti_5Sn_3 with perfect and different vacancies.

Compound	C_{11}	C_{12}	C_{13}	C_{33}	C_{44}	C_{66}
Ti_5Sn_3	192.18	116.80	45.03	220.82	48.02	37.69
Other [a]	182.23	111.22	46.60	199.72	47.43	35.51
V_{Ti1}	194.78	69.61	51.56	190.25	63.25	62.58
V_{Ti2}	204.20	73.12	45.55	191.47	56.63	65.54
V_{Sn3}	165.25	96.14	59.38	182.70	24.57	34.56

[a] Ref. [13].

According to Table 4, through the Voigt-Reuss-Hill (VRH) relation, the elastic constant C_{ij} is used to calculate the macroscopic elastic parameters, such as the volume elastic modulus (B), shear elastic modulus (G) and Poisson's ratio (ν). The formula is as follows:

$$E = \frac{9BG}{3B + G} \tag{8}$$

$$\nu = \frac{3B - 2G}{2(3B + G)} \tag{9}$$

The deformation resistance and elastic strain of the solid are mainly expressed by Vickers hardness, which is one of the important parameters of mechanics. Therefore, the intrinsic hardness of perfect Ti_5Sn_3 and Ti_5Sn_3 with vacancy was studied. Their Vickers hardness can be expressed by the following formula [31,32]:

$$H_v = 2((G/B)^2 \cdot G)^{0.585} - 3 \tag{10}$$

Various macroscopic elastic parameters calculated are listed in Table 5. It can be seen from Table 5 that the bulk modulus of Ti_5Sn_3 with vacancy is smaller than that of perfect Ti_5Sn_3. This indicates that the removal of Ti and Sn atoms can weaken the volumetric deformations resistance of the crystal. In addition, the Ti vacancy can enhance the shear deformation resistance and stiffness of Ti_5Sn_3, because the shear modulus and Young's modulus of Ti_5Sn_3 with Ti vacancy are greater than those of intact Ti_5Sn_3. Consistent with the shear modulus and Young's modulus, the Vickers hardness of Ti vacancy Ti_5Sn_3 is greater than that of perfect Ti_5Sn_3, indicating that the Ti vacancy leads to the increase in Vickers hardness of Ti_5Sn_3. The value of Poisson's ratio is generally between 0~0.5. The greater the hardness of the material, the smaller the Poisson's ratio; On the contrary, the softer the material, the greater the Poisson's ratio, which is fully proved by the data of Poisson's ratio and hardness in Table 5. According to Pugh's empirical rule [33–35], if the value of B/G is less than 1.75, the material has ductility, otherwise it does not. Obviously, the Pugh ratio of complete Ti_5Sn_3 obtained from Table 5 is 2.24, which is ductile, and the B/G of Sn vacancy Ti_5Sn_3 is 4.04, indicating that the Sn vacancy can improve the ductility of the material. However, Ti vacancy Ti_5Sn_3 is less than 1.75, indicating that the Ti vacancy can reduce the ductility of Ti_5Sn_3. Compared with Ti vacancy, Sn vacancy has a greater influence on Ti_5Sn_3. It can be clearly seen from Table 5 that the removal of Sn atom greatly reduces the shear modulus, Young's modulus and hardness of Ti_5Sn_3.

Table 5. Volume modulus (B), shear modulus (G), Young's modulus (E), Poisson's ratio (ν) and intrinsic hardness (H_v) of perfect and different vacancy Ti_5Sn_3.

Compound	B (GPa)	G (GPa)	E (GPa)	B/G	ν	H_v (GPa)
Ti_5Sn_3	112.85	50.39	131.58	2.24	0.31	10.91
Other [a]	108.11	50.06	124.60	2.26	0.31	
V_{Ti1}	99.21	61.19	152.27	1.62	0.24	15.82
V_{Ti2}	103.08	63.28	157.59	1.63	0.25	16.14
V_{Sn3}	103.74	25.71	71.24	4.04	0.38	3.64

[a] Ref. [13].

3.3. Electronic Structure

In order to further study the chemical bonding and mechanical properties of Ti_5Sn_3 with different vacancies, densities of states of perfect Ti_5Sn_3 and Ti_5Sn_3 with different vacancies were calculated in this paper, as shown in Figure 3 below. The dotted line positions indicate the Fermi energy levels. It can be seen that the density of states of perfect Ti_5Sn_3 and Ti_5Sn_3 with different vacancies are very similar. Obviously, in Figure 3a, from −10.6 eV to −6.2 eV, the 5s state of Sn atom plays a major role. From −5.9 eV to the Fermi level, the density of this region is mainly contributed by Sn–5p and Ti–3d, and Sn–5p and Ti–3p also have a small contribution. In addition, charge transfer from the Sn–4s state to the 3p state occurs in this part. To the right of the Fermi level, the density of this segment is mainly contributed by Ti–3d, and there is a large overlap in this range, which indicates that there is a strong orbital hybridization between Ti and Sn, and between Ti and Ti, forming the Ti–Sn and Ti–Ti bonds. In addition, it can be seen from Figure 3b–d that the vacancy causes the valley phase change near the Fermi level. Ti vacancy makes the valley phase transition shallow, and Sn vacancy makes the valley phase increase significantly. As shown in Figure 3c, for V_{Ti2}, the density of states forms a small peak at the Fermi level, which indicates that the removal of Ti atoms at the V_{Ti2} position is conducive to the interaction between charges, which strengthens the Ti–Sn bond. For V_{Sn3}, the density of states forms a valley phase at the Fermi level, indicating that the interatomic hybridization between Ti and Sn is weakened and the Ti–Sn bond is weakened.

It is well known that vacancies alter chemical bonding states and mechanical properties. In order to better explore the chemical bonding characteristics and mechanical properties of Ti_5Sn_3 and different vacant Ti_5Sn_3, this paper calculated their charge density difference respectively, as shown in Figure 4. Blue represents the absence of electrons, red represents the enrichment of electrons, and white represents no change in electron density. It can be seen from Figure 4a that on the (001) plane, electron deletion mainly occurs around Sn atoms and electron enrichment mainly occurs around Ti atoms, indicating the formation of Ti-Sn bond. For perfect Ti_5Sn_3, the Ti1–Sn, Ti2–Sn and Ti2–Ti2 bonds on (001) plane is 2.766 Å, 2.840 Å and 2.725 Å, respectively (as shown in Table 6). For the vacancy of Sn, the removal of the Sn atom weakens the bonding strength and hybridization between the Sn atom and Ti atom, so the deformation resistance becomes weak, which is also the reason for the decrease in the elastic modulus. It can be seen from Table 6 that the Ti vacancy, especially the removal of Ti atoms at the V_{Ti2} position, is conducive to the improvement of the strength of Ti–Sn bond and Ti–Ti, which indicates that the interaction between Ti atoms and between Ti atoms and Sn atoms is enhanced.

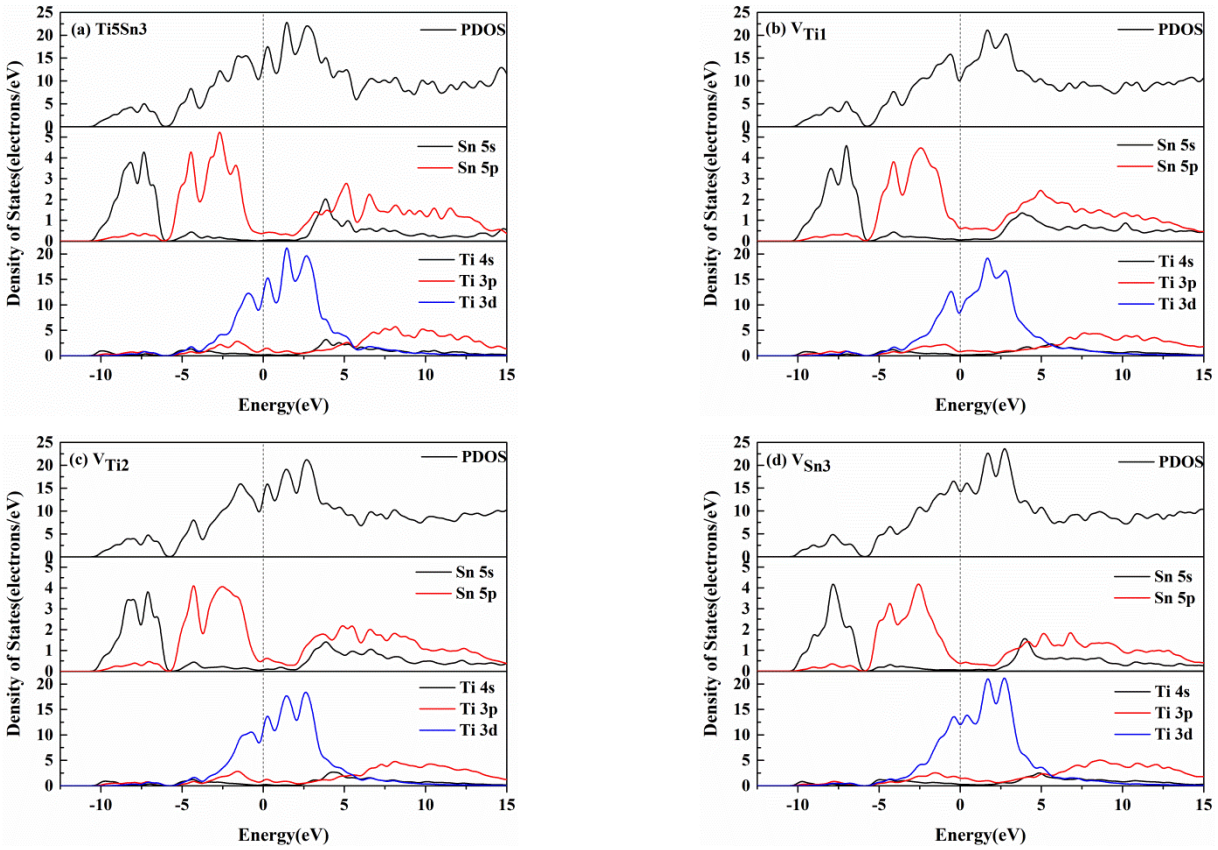

Figure 3. The total and partial density of states (DOS) of Ti_5Sn_3 with different vacancies, (**a**) Ti_5Sn_3, (**b**) V_{Ti1}, (**c**) V_{Ti2} and (**d**) V_{Sn3}, respectively.

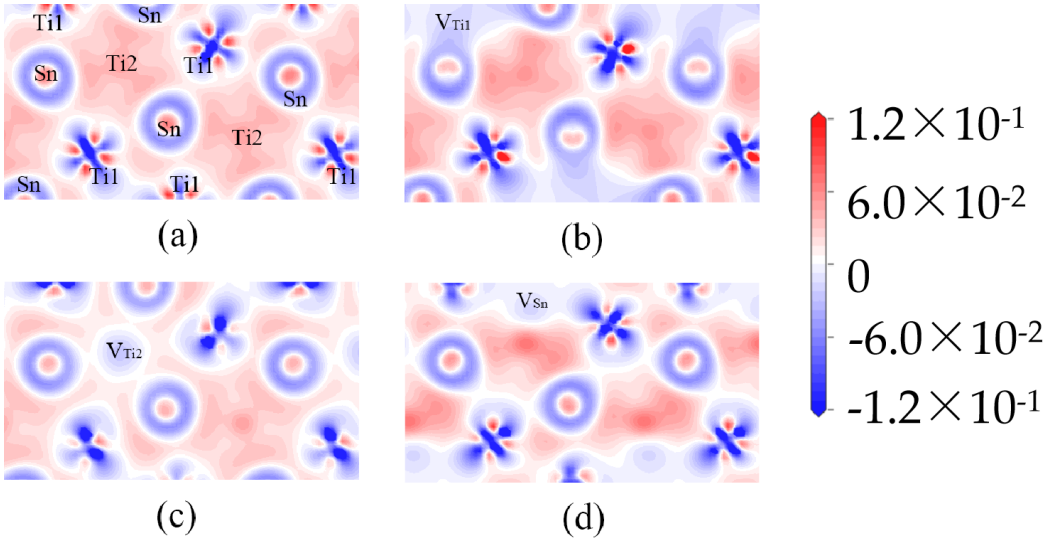

Figure 4. The difference charge density contour plots of Ti_5Sn_3 with four different vacancies along the (0 0 1) plane. (**a**) Ti_5Sn_3, (**b**) V_{Ti1}, (**c**) V_{Ti2}, and (**d**) V_{Sn}, respectively.

Table 6. The bond lengths in the (0 0 1) surface of Ti_5Sn_3 with different vacancies.

Bonds	Ti_5Sn_3 (Å)	V_{Ti1} (Å)	V_{Ti2} (Å)	V_{Sn3} (Å)
Ti1-Sn	2.766	2.836	2.758	2.873
Ti2-Sn	2.840	2.890	2.840	2.899
Ti2-Ti2	2.725	2.699	2.720	2.729

4. Conclusions

In this paper, the mechanical properties and electronic structures of perfect Ti_5Sn_3 and different vacant Ti_5Sn_3 are studied by using first-principles calculations. The comprehensive calculation results draw the following conclusions:

(1) According to vacancy formation energy and vacancy formation enthalpy, Ti vacancy has better structural stability than Sn vacancy, and Ti_5Sn_3 is more inclined to form vacancy at V_{Ti2}.
(2) According to the calculation results of elastic properties, the vacancy weakens the bulk deformation capacity of Ti_5Sn_3, and the Ti vacancy increases the shear resistance, stiffness and hardness of Ti_5Sn_3, while the vacancy of Sn is the opposite.
(3) Ti vacancy can increase the brittleness of Ti_5Sn_3, while Sn vacancy can strengthen the toughness of Ti_5Sn_3.
(4) The changes in electronic structure and chemical bonds indicate that the removal of the Ti atom at the V_{Ti2} position can strengthen the interatomic interaction, while the Sn vacancy will weaken the interaction.

Author Contributions: Conceptualization, X.P.; methodology, D.L. and M.P.; software, F.W.; data curation, W.Y. and J.W.; writing—original draft preparation, X.P.; writing—review and editing, Y.Z. and J.Y. All authors have read and agreed to the published version of the manuscript.

Funding: This research was funded by [Guangxi Natural Science Foundation] grant number [2021GXNSFAA220088, 2021GXNSFBA220080], [Key Projects of Regional Innovative Cooperative Development Foundation from NSFC] grant number [U20A20276], [National Natural Science Foundation of China] grant number [51761002, 51961008], [Special funds for Local Scientific and Technological Development Funds Guided by the Central Government in 2021] grant number [GuiKeZY21195030], [Guangxi Science and Technology Base and Talent Project in 2022] grant number [GuiKeAD21238010], [Scientific Research Project for Xingjian College of Science and Liberal Arts of Guangxi University] grant number [Y2019ZKK01], [the Doctoral Program of Guangxi University] grant number [XBZ200300], [Basic Competence Improvement Project for Middle and Young Teachers in Guangxi Universities] grant number [2017KY0032, 2018KY0784], [National key research and development program] grant number [2018YFC1902802-4], [research project of Guangxi Key Laboratory of Processing for Non-ferrous Metallic and Featured Materials] grant number [2021GXMPSF06], [Science and technology project of General Administration of Customs] grant number [2020HK255], [Shenzhen Science and Technology Project] grant number [JSGG2022301090002002].

Institutional Review Board Statement: Not applicable.

Informed Consent Statement: Not applicable.

Data Availability Statement: Data is contained within the article.

Conflicts of Interest: The authors declare no conflict of interest.

References

1. Niinomi, M. Recent metallic materials for biomedical applications. *Metall. Mater. Trans. A* **2002**, *33*, 477–486. [CrossRef]
2. Long, M.; Rack, H.J. Titanium alloys in total joint replacement-a materials science perspective. *Biomaterials* **1998**, *19*, 1621–1639. [CrossRef]
3. Wang, B.L.; Zheng, Y.F.; Zhao, L.C. Effects of Sn content on the microstructure, phase constitution and shape memory effect of Ti–Nb–Sn alloys. *Mater. Sci. Eng. A* **2008**, *486*, 146–151. [CrossRef]
4. Zhang, X.Z.; Leary, M.; Tang, H.P.; Song, T.; Qian, M. Selective electron beam manufactured Ti-6Al-4V lattice structures for orthopedic implant applications: Current status and outstanding challenges. *Curr. Opin. Solid State Mater. Sci.* **2018**, *22*, 75–99. [CrossRef]
5. Niinomi, M. Recent research and development in titanium alloys for biomedical applications and healthcare goods. *Sci. Technol. Adv. Mater.* **2003**, *4*, 445–454. [CrossRef]
6. Pilliar, R.M. Modern metal processing for improved load-bearing surgical implants. *Biomaterials* **1991**, *12*, 95–100. [CrossRef]
7. Wang, X.; Li, Y.; Xiong, J.; Hodgson, P.D. Porous TiNbZr alloy scaffolds for biomedical applications. *Acta Biomater.* **2009**, *5*, 3616–3624. [CrossRef] [PubMed]
8. Choubey, A.; Balasubramaniam, R.; Basu, B. Effect of replacement of V by Nb and Fe on the electrochemical and corrosion behavior of Ti–6Al–4V in simulated physiological environment. *J. Alloys Compd.* **2004**, *381*, 288–294. [CrossRef]

9. Gutiérrez-Moreno, J.J.; Guo, Y.; Georgarakis, K.; Yavari, A.R.; Evangelakis, G.A.; Lekka, C.E. The role of Sn doping in the β-type Ti–25 at% Nb alloys: Experiment and ab initio calculations. *J. Alloys Compd.* **2014**, *615*, S676–S679. [CrossRef]
10. Moraes, P.E.; Contieri, R.J.; Lopes, E.S.; Robin, A.; Caram, R. Effects of Sn addition on the microstructure, mechanical properties and corrosion behavior of Ti–Nb–Sn alloys. *Mater. Charact.* **2014**, *96*, 273–281. [CrossRef]
11. Hao, Y.L.; Li, S.J.; Sun, S.Y.; Yang, R. Effect of Zr and Sn on Young's modulus and superelasticity of Ti–Nb-based alloys. *Mater. Sci. Eng. A* **2006**, *441*, 112–118. [CrossRef]
12. Ijaz, M.F.; Kim, H.Y.; Hosoda, H.; Miyazaki, S. Superelastic properties of biomedical (Ti–Zr)–Mo–Sn alloys. *Scr. Mater.* **2014**, *72–73*, 29–32. [CrossRef]
13. Colinet, C.; Tedenac, J.C. Constitutional and thermal defects in B82–SnTi2. *Intermetallics* **2009**, *17*, 291–304. [CrossRef]
14. Colinet, C.; Tedenac, J.C. Structural stability of intermetallic phases in the Si–Ti system. Point defects and chemical potentials in D88-Si3Ti5 phase. *Intermetallics* **2010**, *18*, 1444–1454. [CrossRef]
15. Hong, D.; Zeng, W.; Xin, Z.; Liu, F.S.; Tang, B.; Liu, Q.J. First-principles calculations of structural, mechanical and electronic properties of TiNi-X (X = C, Si, Ge, Sn, Pb) alloys. *Int. J. Mod. Phys. B* **2019**, *33*, 1950167. [CrossRef]
16. Künnen, B.; Jeitschko, W.; Kotzyba, G.; Mosel, B.D. Crystal structure and properties of the titanium stannide Ti2Sn3. *Z. Naturforsch. B* **2015**, *55*, 425–430. [CrossRef]
17. Rittiruam, M.; Yangthaisong, A.; Seetawan, T. Enhancing the thermoelectric performance of self-defect TiNiSn: A first-principles calculation. *J. Electron. Mater.* **2018**, *47*, 7456–7462. [CrossRef]
18. Wang, X.F.; Li, W.; Fang, G.P.; Wu, C.W.; Lin, J.G. First-principles calculations on the electronic structure and cohesive properties of titanium stannides. *Intermetallics* **2009**, *17*, 768–773. [CrossRef]
19. Tedenac, J.C.; Yot, P.G.; Bulanova, M.; Fartushna, J.; Colinet, C. Evidence of an ordered ternary phase in the section Ni–Ti5Sn3 of the ternary Ti–Ni–Sn: Crystal structure and phase stability. *Solid State Sci.* **2020**, *109*, 106349. [CrossRef]
20. Chen, X.J.; Mo, Z.S.; Wang, R.N.; Zeng, M.X.; Tang, B.Y.; Peng, L.M.; Ding, W.J. Elastic and electronic properties of the Ti5X3 (X= Si, Ge, Sn, Pb) compounds from first-principles calculations. *J. Solid State Chem.* **2012**, *194*, 127–134. [CrossRef]
21. Segall, M.D.; Lindan, P.J.; Probert, M.A.; Pickard, C.J.; Hasnip, P.J.; Clark, S.J.; Payne, M.C. First-principles simulation: Ideas, illustrations and the CASTEP code. *J. Phys. Condens. Matter* **2002**, *14*, 2717. [CrossRef]
22. Perdew, J.P.; Burke, K.; Ernzerhof, M. Generalized Gradient Approximation Made Simple. *Phys. Rev. Lett.* **1996**, *77*, 3865–3868. [CrossRef] [PubMed]
23. Vanderbilt, D. Soft self-consistent pseudopotentials in a generalized eigenvalue formalism. *Phys. Rev. B* **1990**, *41*, 7892–7895. [CrossRef] [PubMed]
24. Fischer, T.H.; Almlof, J. General methods for geometry and wave function optimization. *Phys. Chem.* **1992**, *96*, 9768–9774. [CrossRef]
25. Pietrokowsky, P.; Duwez, P. Crystal structure of Ti5Si3, Ti5Ge3, and Ti5Sn3. *JOM* **1951**, *3*, 772–773. [CrossRef]
26. Pan, Y.; Li, Y.Q.; Zheng, Q.H.; Xu, Y. Point defect of titanium sesquioxide Ti_2O_3 as the application of next generation Li-ion batteries. *J. Alloys Compd.* **2019**, *786*, 621–626. [CrossRef]
27. Colinet, C.; Tedenac, J.C.; Fries, S.G. Structural stability of intermetallic phases in the Sn–Ti system. *Calphad* **2008**, *33*, 250–259. [CrossRef]
28. Yang, J.; Pang, X.; Han, J.; Pang, M.; Wei, F.; Yang, W.; Zhan, Y. Influence of vacancy on the mechanical behavior, thermodynamic properties and electronic structure of orthorhombic Ti3Sn from first-principles calculations. *Vacuum* **2021**, *188*, 110178. [CrossRef]
29. Lv, Y.; Zhang, X.; Jiang, W. Phase stability, elastic, anisotropic properties, lattice dynamical and thermodynamic properties of B12M (M = Th, U, Np, Pu) dodecaborides. *Ceram. Int.* **2018**, *44*, 128–135. [CrossRef]
30. Quan, S.; Liu, C.; Jiang, W.; Zhang, X. First-principles investigation of the mechanical, anisotropic and thermodynamic properties of RET2Al20 (RE = La, Ce, Gd, T = Ti, V) intermetallics. *Phys. B Condens. Matter.* **2019**, *554*, 64–71. [CrossRef]
31. Li, L.H.; Wang, W.L.; Hu, L.; Wei, B.B. First-principle calculations of structural, elastic and thermodynamic properties of Fe–B compounds. *Intermetallics* **2014**, *46*, 211–221. [CrossRef]
32. Zhang, X.; Dong, T.; Ma, H.; Li, D.; Ying, C.; Liu, C.; Wang, F. A first principles investigation on the influence of transition-metal elements on the structural, mechanical, and anisotropic properties of CaM2Al20 intermetallics. *J. Mol. Graph. Model* **2019**, *96*, 107509. [CrossRef] [PubMed]
33. Pugh, S.F. XCII. Relations between the elastic moduli and the plastic properties of polycrystalline pure metals. *Phil. Mag. J. Sci* **1954**, *45*, 823–843. [CrossRef]
34. Yıldız, G.D.; Yıldız, Y.G.; Al, S.; İyigör, A.; Arıkan, N. Computational investigations of mechanic, electronic and lattice dynamic properties of yttrium based compounds. *Int. J. Mod. Phys. B* **2018**, *32*, 1850214. [CrossRef]
35. Al, S.; Arikan, N.; Iyigör, A. Investigations of structural, elastic, electronic and thermodynamic properties of X2TiAl Alloys: A computational study. *Z. Naturforsch. A* **2018**, *73*, 859–867. [CrossRef]